Journal of Applied Physics

RESEARCH ARTICLE | DECEMBER 19 2023

Diffusion-controlled annealing kinetics of interstitial H in SnO_2

Special Collection: Defects in Semiconductors 2024

Andrew Venzie ; Michael Stavola ; W. Beall Fowler ; Lynn A. Boatner

J. Appl. Phys. 134, 235704 (2023)
https://doi.org/10.1063/5.0186047

Journal of Applied Physics ARTICLE pubs.aip.org/aip/jap

Diffusion-controlled annealing kinetics of interstitial H in SnO_2

Cite as: J. Appl. Phys. **134**, 235704 (2023); doi: 10.1063/5.0186047
Submitted: 3 November 2023 · Accepted: 25 November 2023 ·
Published Online: 19 December 2023

Andrew Venzie,[1] Michael Stavola,[1,a)] W. Beall Fowler,[1] and Lynn A. Boatner[2]

AFFILIATIONS

[1]Department of Physics, Lehigh University, Bethlehem, Pennsylvania 18015, USA
[2]Oak Ridge National Laboratory, Materials Science and Technology Division, Oak Ridge, Tennessee 37831, USA

Note: This paper is part of the special topic, Defects in Semiconductors 2024.
[a)]**Author to whom correspondence should be addressed:** michael.stavola@Lehigh.edu

ABSTRACT

SnO_2 is a prototypical transparent conducting oxide that finds widespread applications as transparent electrodes, gas sensors, and transparent thin-film devices. Hydrogen impurities in SnO_2 give rise to unintentional n-type behavior and unexpected changes to conductivity. Interstitial H (H_i) and H at an oxygen vacancy (H_O) are both shallow donors in SnO_2. An O–H vibrational line at 3155 cm^{-1}, that can be produced by a thermal anneal at 500 °C followed by a rapid quench, has been assigned to the H_i center and is unstable at room temperature on a timescale of weeks. An IR absorption study of the decay kinetics of the 3155 cm^{-1} O–H line has been performed. The disappearance of H_i upon annealing has been found to follow second-order kinetics. Measurements of the decay rate for a range of temperatures have determined an activation energy for the diffusion of interstitial H in SnO_2. These results provide fundamental information about how unintentional hydrogen impurities and their reactions can change the conductivity of SnO_2 device materials in processes as simple as thermal annealing in an inert ambient.

I. INTRODUCTION

Transparent conducting oxides (TCOs) are wide bandgap semiconductors that combine transparency in the visible region of the spectrum with high conductivity.[1–3] SnO_2, with its rutile crystal structure and bandgap energy of 3.6 eV,[4] is a classic example. For decades, oxide semiconductors like SnO_2 have found broad application as transparent electrodes, gas sensors, transparent thin-film transistors, and energy-saving coatings for windows.[1–9] Nonetheless, the background n-type conductivity of TCOs remains difficult to understand and control.

Hydrogen impurities in SnO_2 give rise to n-type conductivity,[10] consistent with a modern understanding of the unintentional conductivity of a variety of TCOs[11–16] that continues to be investigated. Theory found that interstitial hydrogen (H_i) and hydrogen at an oxygen vacancy (H_O) are shallow donors in SnO_2,[17] a prediction that proved to be consistent with subsequent experiments.[18,19] Furthermore, muon-spin-rotation (μSR) measurements have found that muonium centers that mimic the properties of H in semiconductors give rise to shallow donors that are mobile below room temperature.[20–22]

An O–H vibrational line observed in SnO_2 at 3155 cm^{-1} was assigned to H_i, whose structure consists of a single H attached to a threefold coordinated O such that the O–H transition dipole direction is perpendicular to the crystal c axis.[18,19] Thermally stable conductivity has been associated with the H_O center. Several additional OH–X centers that involve an additional defect or impurity were also discovered.[18,19,23] Both Sn vacancies and interstitial defects have been suggested as candidates for the accompanying defects labeled generically as X.[18,19,24,25] O–H centers that contain more than one H atom were also discovered.[19]

It is not uncommon in TCOs for H to be exchanged between defects that have different electrical activities, with an example being the dissociation of H_2 in ZnO to give rise to electrically active H_i centers.[26,27] In this way, an electrically inactive defect can act as a source or sink for H in reactions that affect the conductivity of device materials.

In SnO_2, it was found that the H_i shallow donor introduced by annealing in an H_2 ambient is mobile at room temperature, and electrically inactive XH centers were formed on a timescale of weeks.[18,19] Furthermore, hydrogen was also found to be released

from an electrically inactive source that could be converted into electrically active H_i centers by annealing treatments in an inert ambient.[18,19] Such hydrogen-related reactions make the conductivity of oxide device materials difficult to control in processes as simple as thermal annealing in an inert ambient.

In the present paper, vibrational spectroscopy[28,29] is used to investigate the annealing behavior of H_i in SnO_2 as an example of a hydrogen-defect reaction that changes the conductivity of a model TCO. The role of hydrogen diffusion in the annealing kinetics of H_i is a focus of this study.

II. EXPERIMENTAL METHODS

The SnO_2 samples used in our experiments were bulk, rutile-phase single crystals grown by the vapor transport method.[30] Fortunately, the as-grown crystals contained a sufficient concentration of H for our studies, which had a few advantages. The as-grown crystals showed an O–H spectrum with fewer lines than had been reported previously for samples annealed in an H_2 ambient. Defects containing two H atoms and a recently reported electrically active O–H center[31] with a vibrational line at 3272 cm^{-1} are absent, which simplifies the defect reactions that occur in our experiments. Furthermore, anneals in an H_2 ambient leave a layer of tin on the sample surface, an effect we were able to avoid by using as-grown samples that contained H.

IR absorption spectra were measured with a Nicolet iS50 Fourier-transform-infrared spectrometer equipped with a CaF_2 beam splitter and a liquid N_2 cooled InSb detector. The polarization of the transmitted light was analyzed with a wire-grid polarizer placed after the sample. The O–H spectral features studied here were all observed for the polarization **E** perpendicular to **c**. Samples were cooled for our measurements with liquid N_2 in a Helitran continuous flow cryostat. Annealing treatments were performed in a tube furnace in a flowing Ar ambient.

III. RESULTS

Figure 1 shows absorbance spectra (77 K, 1 cm^{-1} resolution) for a SnO_2 sample that contained H that had been introduced during crystal growth. To initiate the series of sequential anneals whose resulting spectra are shown in Fig. 1, a sample was annealed in an Ar ambient at 500 °C for 30 min and then quenched to room temperature in H_2O. This treatment produced the O–H line at 3155 cm^{-1} that has been assigned previously to H_i as well as additional O–H lines at 3174, 3256, 3270, and 3298 cm^{-1} that have been assigned to XH complexes.[18,19] In the selection of spectra shown in Fig. 1, the line at 3155 cm^{-1} can be seen to decrease in intensity upon subsequent annealing at 80 °C [Fig. 1(a)] while the lines at 3256, 3270, and 3298 cm^{-1} increase in intensity [Fig. 1(b)]. (H_O centers in SnO_2 have been found to be thermally stable at the 500 °C temperature we have used to initiate an annealing sequence,[19] and also during subsequent anneals at lower temperatures, and are not important in our experiments.)

The integrated areas of the O–H absorbance lines can be converted to a concentration of O–H centers with the relationship given in Eq. (1),[28]

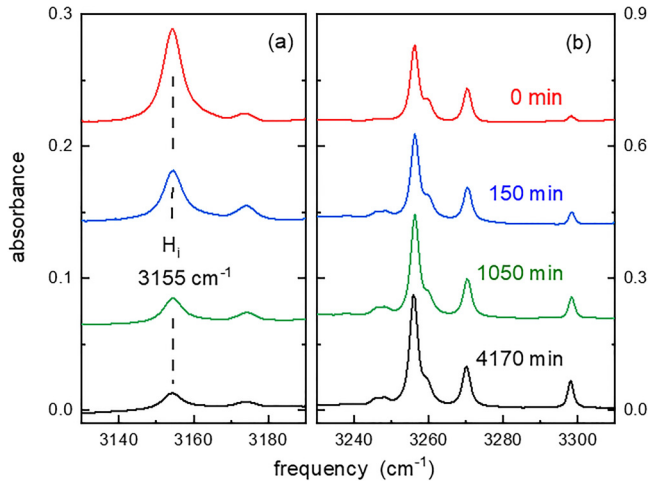

FIG. 1. IR absorption spectra (77 K, resolution = 0.5 cm^{-1}, polarization **E** perpendicular to **c**) for a SnO_2 sample annealed in an Ar ambient (500 °C, 30 min) to produce interstitial H. This sample was subsequently annealed at 80 °C for the indicated times (in min). (a) The annealing behavior of the O–H line at 3155 cm^{-1} assigned to interstitial H. (b) The O–H lines assigned to XH complexes that form upon annealing at 80 °C.

$$N = [(2.303\ nc^2m)/(\pi q^2 d)]\int A(\bar{\upsilon})d\bar{\upsilon}. \quad (1)$$

Here, $A(\bar{\upsilon})$, is the absorbance as a function of frequency in wavenumber units, d is the thickness of the sample, m is the reduced mass of the oscillating defect, c is the speed of light, and n is the refractive index. In Eq. (1), q is an "effective charge" that must be determined by an independent calibration of a defect's concentration. For an approximate calibration for the O–H centers in SnO_2, we use the value $q = 0.30e$ that is typical of the effective charges determined recently for O–H centers in ZnO and Ga_2O_3.[32,33] While uncertainties in the values of effective charges for defects can be near a factor of 2 or more, they provide a strategy for making an order-of-magnitude estimate of a defect's concentration from its IR spectrum.

The change in the concentrations of O–H centers that occurs upon annealing at 80 °C is plotted in Fig. 2(a). Results for H_i are shown as black circles, and the sum of the areas for the lines at 3256, 3270, and 3298 cm^{-1} lines assigned to XH complexes are shown as blue squares. The annealing spectra are characteristic of a reaction where interstitial H becomes trapped by another defect X,

$$H_i + X \rightleftarrows XH. \quad (2)$$

Treating the 3256, 3270, and 3298 cm^{-1} centers together as H_i trapped by a generic defect X provides a model that adequately explains our experimental results.

The curves in Fig. 2(a) compare fits with first- and second-order kinetics for the disappearance of H_i upon annealing. It can be seen that a second-order rate law,[34,35] Eq. (3), provides a better

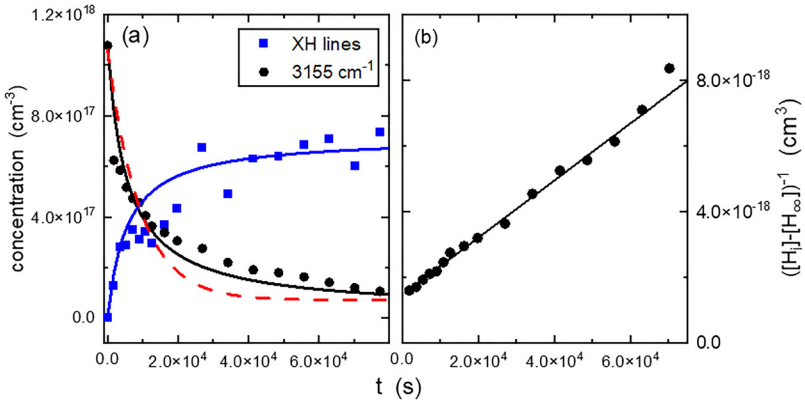

FIG. 2. (a) Plot of concentration, $[H_i(t)]$, vs annealing time (black) at 80 °C for the IR line at 3155 cm^{-1} assigned to H_i. Included also is a plot of the change in total concentration of XH complexes (blue) vs annealing time. The dashed red trace is a fit with first-order kinetics. The black trace is a fit with second-order kinetics. The blue trace shows the total concentration of XH centers plotted with the same second-order rate constant found from the fit for the decay of the 3155 cm^{-1} line. (b) Plot of $([H_i(t)] - [H_\infty])^{-1}$ vs the annealing time at 80 °C for the IR line at 3155 cm^{-1}.

description of our data than first-order kinetics does

$$[H_i(t)] - [H_\infty] = [H_0]/([H_0]kt + 1). \tag{3}$$

Here, $[H_0]$ is the initial concentration of H_i and $[H_\infty]$ is the concentration of H_i at long annealing times. A bimolecular rate law is expected for a reaction like Eq. (2) if the concentrations of H_i and X are approximately equal. It is often the case that the concentration of H introduced into a semiconductor mimics the concentration of a defect where it becomes trapped, as seems to be the case here.[36] Figure 2(b) shows a plot of $([H_i(t)] - [H_\infty])^{-1}$ vs the annealing time; the approximately linear relationship that results is also a well-known signature of second-order kinetics.[34,35] The slope of the linear fit shown in Fig. 2(b) is the second-order rate constant k in Eq. (3).

The O–H line at 3155 cm^{-1} could be regenerated by an additional annealing treatment at 500 °C followed by a rapid quench to room temperature. The annealing kinetics for the decay of H_i were then measured for several temperatures between 20 and 120 °C. Figure 3(a) shows a plot of $([H_i(t)] - [H_\infty])^{-1}$ vs the annealing time for a few selected temperatures. Similar to the results shown in Fig. 2(b), the second-order rate law in Eq. (3) provides a satisfactory fit to these data.

In the 1950s, Reiss *et al.*[37] and Reiss[38] studied ion-pairing reactions that involved Li and acceptor impurities in Ge. These reactions were found to be limited by the diffusivity of the light Li^+ ion. We postulate that the situation is similar here and that the pairing reaction in Eq. (2) is limited by the diffusivity of the light H_i^+ ion. If we assume that the second-order rate constant k is proportional to the product of a capture radius R_0 for the XH complex and the diffusivity of H_i, the slope of a plot of $\ln(k)$ vs T^{-1} yields E_A/k_B. We have also taken the diffusivity to obey a standard Arrhenius relationship and for R_0 to be independent of temperature. The fit to the data plotted in Fig. 4 (shown in black) gives an activation energy for H_i diffusion in SnO_2 of 0.53 ± 0.05 eV.

Also in the 1950s, Waite developed a theory for second-order diffusion-controlled reactions[39] that he applied to the recombination of radiation defects in Ge.[40] Waite's model has been used successfully by chemists to analyze the annealing of radiation damage in polymers.[41] In Waite's analysis, he considered the fraction of unreacted vacancy-interstitial pairs, φ, and found that for early annealing times,

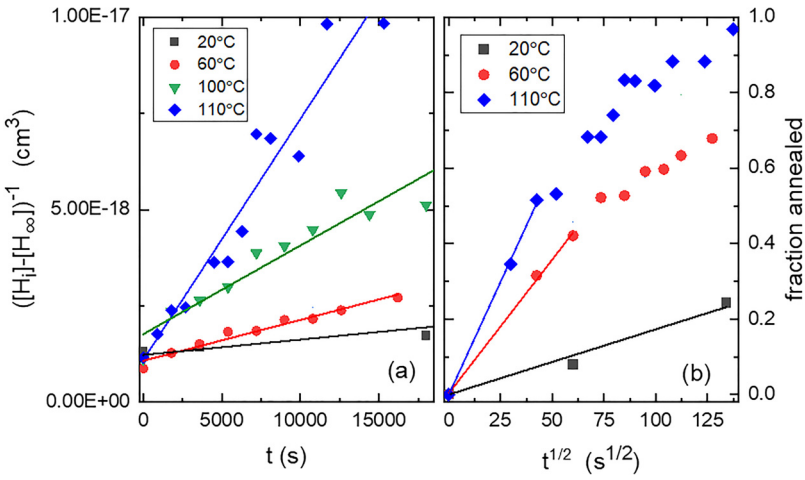

FIG. 3. (a) Plot of $([H_i(t)] - [H_\infty])^{-1}$ vs the annealing time for different annealing temperatures. (b) Plot of the "fraction annealed" for the H_i center in SnO_2 vs the square root of the annealing time for different annealing temperatures.

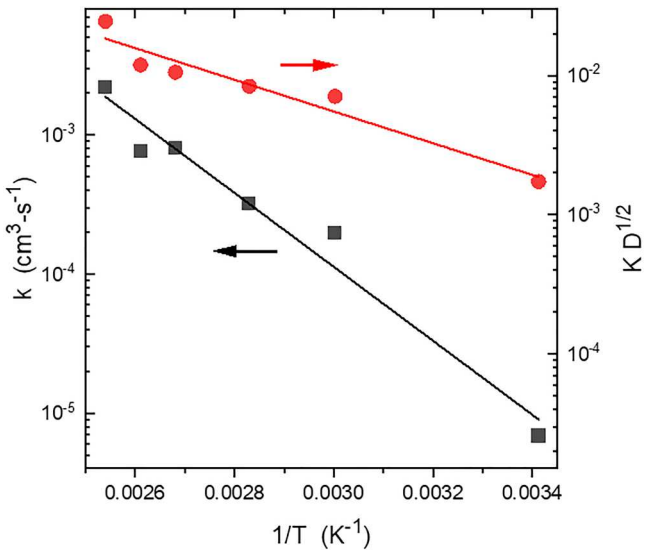

FIG. 4. The second-order rate constant k is the slope of a plot of $([H_i(t)] - [H_\infty])^{-1}$ vs the annealing time shown in Fig. 3(a). A plot (left axis, black) of ln(k) vs 1/T, with slope E_A/k_B, is shown. K $D^{1/2}$ is the slope, at early time, of the "fraction annealed" vs (annealing time)$^{1/2}$ is shown in Fig. 3(b). A plot (right axis, red) of ln(K $D^{1/2}$) vs T^{-1}, with slope $E_A/2k_B$, is shown.

$$\varphi = K(Dt)^{1/2}, \tag{4}$$

where K is a constant that is proportional to the square of the capture radius R_0.[39,40]

The situation in our experiments is similar to that analyzed by Waite.[40] An anneal at 500 °C produces dissociated H_i-X pairs that recombine in a diffusion-controlled reaction to form XH complexes upon annealing. The fraction of unreacted pairs in our case is given by

$$\varphi = ([H_0] - [H_i])/([H_0] - [H_\infty]). \tag{5}$$

A plot of φ vs $t^{1/2}$ is shown in Fig. 3(b) and yields a linear plot for small t, consistent with Eq. (4). In Fig. 3(b), the slope of the plot at small t is proportional to $D^{1/2}$. If Arrhenius behavior is again assumed for the diffusivity, a plot of the ln of the slopes shown in Fig. 3(b) vs T^{-1} yields $E_A/2k_B$ and the value $E_A = 0.45 \pm 0.06$ eV [see Fig. 4 (shown in red)]. This value, obtained with the strategy proposed by Waite, differs from that obtained above by only 0.08 eV.

To make a rough estimate for the diffusivity of interstitial hydrogen, the penetration depth of D upon annealing in a D_2 ambient was investigated. (The D isotope was used because as-grown samples contained no D above its small natural isotopic abundance for hydrogen.) A SnO_2 sample was annealed in a D_2 ambient in a sealed ampoule for 30 min at 500 °C. This sample was then thinned in steps by lapping and polishing. IR measurements showed that O–D centers were eliminated when a layer of thickness d = 0.035 mm had been removed from the sample surface. This result yields a diffusion constant of $D(500\,°C) = d^2/t = 6.8 \times 10^{-9}$ cm^2/s. If we take $E_A = 0.45$ eV and assume that the penetration depths for H and D are similar, the diffusivity of H_i in SnO_2 is

$$D = 6 \times 10^{-6}\ \mathrm{cm^2/s}\ \exp(-0.45\ \mathrm{eV/kT}). \tag{6}$$

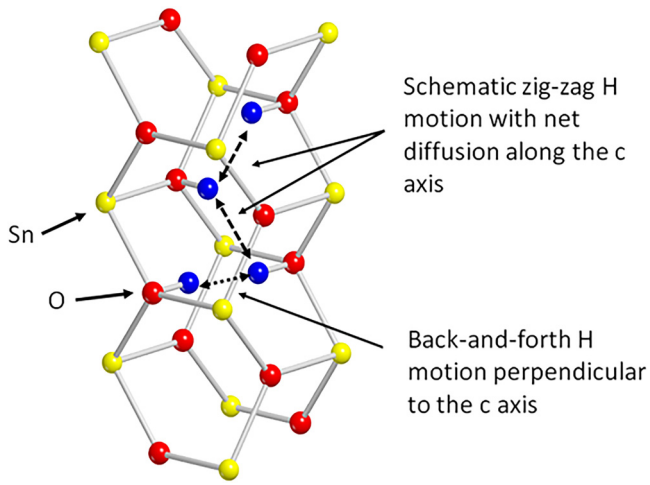

FIG. 5. Schematic illustration of H_i motion in SnO_2. A similar situation occurs for H_i in TiO_2. This figure was constructed using MOLDRAW[42] and POV-Ray.[43].

IV. DISCUSSION

As noted in Sec. I, the structure of H_i in SnO_2 consists of a single H attached to a threefold coordinated O such that the O–H bond is perpendicular to the c axis. Such sites are shown in Fig. 5.

In addition to studying H in SnO_2,[19,25] Bekisli *et al.*[44] carried out research on H in TiO_2, which shares the same rutile structure as SnO_2. Research on H in TiO_2 has been extensive, going back to diffusion studies by Johnson *et al.*[45] and vibrational studies by Bates *et al.*,[46,47] as well as theoretical work by Filippone *et al.*,[48] Marinopoulos *et al.*,[49] and others.[50] This earlier work explains the diffusion of H along the c axis of TiO_2 as a zig-zag or helical motion with an experimental activation energy of 0.59 eV as well as a fundamental O–H stretch frequency of 3286 cm^{-1} with a transition dipole perpendicular to the c axis. It was noted as well[47,49] that the experimental activation energy will be less than the barrier height by zero-point energy corrections that are of order 0.2 eV.

Because the defect structure of H_i in SnO_2 is similar to that in TiO_2, it is reasonable to compare the two cases. Indeed, computed barrier heights for c axis diffusion[17,48,49] are similar as are the experimental values of activation energy for c axis diffusion, vibrational frequency, and O–H_i dipole direction. Applying an estimated zero-point correction of 0.2 eV to our measured activation energy (0.45–0.53 eV) for H_i yields a barrier height of 0.65–0.73 eV, somewhat larger than theoretically predicted[17] but in the same region.

Thus, this comparison of H_i in TiO_2 and in SnO_2 indicates similar physics for the structure and motion of H_i. It is anticipated that similar correspondences will occur for H_i in other stishovite oxides such as rutile SiO_2.

V. CONCLUSION

Hydrogen is readily introduced into SnO_2 unintentionally during crystal growth and device processing where it gives rise to an interstitial H_i shallow donor center that is mobile at room temperature.[18,19] Annealing treatments of SnO_2 that contains H can convert electrically active H_i centers into electrically inactive XH centers, where X is a generic trap for H, and vice versa. The activation energy for H_i diffusion along the c axis (Fig. 5) has been determined to be near 0.5 eV from the ion-pairing reaction of H_i^+ with other unintentional defects in as-grown SnO_2. These results for the prototypical TCO SnO_2 provide a model system for how hydrogen impurities and their diffusion-controlled reactions can give rise to unexpected changes in conductivity in transparent thin-film device materials.

Note added in proof. Two papers have recently appeared where the activation energy for the diffusion of interstitial H in SnO_2 and TiO_2 were determined by a stress-induced dichroism method.[51,52]

ACKNOWLEDGMENTS

The work at Lehigh University was supported by the National Science Foundation (NSF) (Grant No. DMR 1901563). Portions of this research were conducted on Research Computing resources provided by Lehigh University supported by the NSF (Award No. 2019035).

AUTHOR DECLARATIONS

Conflict of Interest

The authors have no conflicts to disclose.

Author Contributions

Andrew Venzie: Investigation (equal); Methodology (equal); Writing – review & editing (equal). **Michael Stavola:** Conceptualization (equal); Funding acquisition (equal); Investigation (equal); Methodology (equal); Project administration (equal); Resources (equal); Supervision (equal); Writing – original draft (equal). **W. Beall Fowler:** Formal analysis (equal); Investigation (equal); Software (equal); Visualization (equal); Writing – review & editing (equal). **Lynn A. Boatner:** Investigation (equal); Methodology (equal); Resources (equal); Writing – review & editing (equal).

DATA AVAILABILITY

The data that support the findings of this study are available from the corresponding author upon reasonable request.

REFERENCES

[1] *Oxide Semiconductors*, edited by B. G. Svensson, S. J. Pearton, and C. Jagadish (Academic Press, San Diego, 2013).
[2] R. Catlow and A. Walsh, "Semiconducting oxides," J. Phys.: Condens. Matter. **23**, 330301 (2011).
[3] G. Thomas, Nature **389**, 907 (1997).
[4] M. Batzill and U. Diebold, Prog. Surf. Sci. **79**, 47 (2005).
[5] N. Bârsan and U. Weimar, J. Phys.: Condens. Matter. **15**, R813 (2003).
[6] H. A. Klasens and H. Koelmans, Solid State Electron. **7**, 701 (1964).
[7] R. E. Presley, C. L. Munsee, C.-H. Park, D. Hong, J. F. Wager, and D. A. Keszler, J. Phys. D: Appl. Phys. **37**, 2810 (2004).
[8] A. K. Ghosh, C. Fishman, and T. Feng, J. Appl. Phys. **50**, 3454 (1979).
[9] T. Minami, Semicond. Sci. Technol. **20**, S35 (2005).
[10] S. Samson and C. G. Fonstad, J. Appl. Phys. **44**, 4618 (1973).
[11] C. G. Van de Walle, Phys. Rev. Lett. **85**, 1012 (2000).
[12] A. Janotti and C. G. Van de Walle, Nat. Mater. **6**, 44 (2007).
[13] P. D. C. King and T. D. Veal, J. Phys.: Condens. Matter. **23**, 334214 (2011).
[14] M. D. McCluskey, M. C. Tarun, and S. T. Teklemichael, J. Mater. Res. **27**, 2190 (2012).
[15] J. L. Lyons, A. Janotti, and C. G. Van de Walle, in *Oxide Semiconductors*, edited by B. G. Svensson, S. J. Pearton, and C. Jagadish (Academic Press, San Diego, 2013), p. 1.
[16] M. Stavola, W. B. Fowler, Y. Qin, P. Weiser, and S. J. Pearton, in *Ga_2O_3, Technology, Devices, and Applications*, edited by S. J. Pearton, F. Ren, and M. Mastro (Elsevier, Amsterdam, 2018), Chap. 9, p. 191.
[17] A. K. Singh, A. Janotti, M. Scheffler, and C. G. Van de Walle, Phys. Rev. Lett. **101**, 055502 (2008).
[18] W. M. Hlaing Oo, S. Tabatabaei, M. D. McCluskey, J. B. Varley, A. Janotti, and C. G. Van de Walle, Phys. Rev. B **82**, 193201 (2010).
[19] F. Bekisli, M. Stavola, W. B. Fowler, L. Boatner, E. Spahr, and G. Lüpke, Phys. Rev. B **84**, 035213 (2011).
[20] P. D. C. King, R. L. Lichti, Y. G. Celebi, J. M. Gil, R. C. Vilão, H. V. Alberto, J. P. Durte, D. J. Payne, R. B. Egdell, I. McKenzie, C. F. McConville, S. F. J. Cox, and T. D. Veal, Phys. Rev. B **80**, 081201(R) (2009).
[21] B. B. Baker, Y. G. Celebi, R. L. Lichti, H. N. Bani-Salameh, P. W. Mengyan, and B. R. Carroll, Phys. Procedia **30**, 101 (2012).
[22] B. B. Baker, "Charged muonium diffusion in indium oxide and other transparent conducting oxides," Ph.D. dissertation (Texas Tech University, 2015).
[23] R. S. Katiyar, P. Dawson, M. M. Hargreave, and G. R. Wilkinson, J. Phys. C **4**, 2421 (1971).
[24] J. B. Varley, H. Peelaers, A. Janotti, and C. G. Van de Walle, J. Phys.: Condens. Matter. **23**, 334212 (2011).
[25] F. Bekisli, W. B. Fowler, M. Stavola, L. Boatner, E. Spahr, and G. Lupke, Phys. Rev. B **86**, 085206 (2012).
[26] G. A. Shi, M. Saboktakin, M. Stavola, and S. J. Pearton, Appl. Phys. Lett. **85**, 5601 (2004).
[27] E. V. Lavrov, F. Herklotz, and J. Weber, Phys. Rev. Lett. **102**, 185502 (2009).
[28] M. Stavola, in *Identification of Defects in Semiconductors*, edited by M. Stavola (Academic, Boston, 1998), Chap. 3, p. 153.
[29] M. Stavola and W. B. Fowler, J. Appl. Phys. **123**, 161561 (2018).
[30] B. Thiel and R. Helbig, J. Crystal Growth **32**, 259 (1976).
[31] F. Herklotz, I. Chaplygin, E. V. Lavrov, and V. F. Agekyan, Appl. Phys. Lett. **114**, 152103 (2019).
[32] E. V. Lavrov, F. Herklotz, and J. Weber, Phys. Rev. B **79**, 165210 (2009).
[33] A. Karjalainen, P. M. Weiser, I. Makkonen, V. M. Reinertsen, L. Vines, and F. Tuomisto, J. Appl. Phys. **129**, 165702 (2021).
[34] P. Atkins, J. de Paula, and J. Keeler, *Physical Chemistry*, 11th ed. (Oxford University Press, Oxford, 2018).
[35] K. A. Connors, *Chemical Kinetics, The Study of Reaction Rates in Solution* (VCH Publishers, New York, 1990).
[36] S. J. Pearton, J. W. Corbett, and M. Stavola, *Hydrogen in Crystalline Semiconductors* (Springer-Verlag, Heidelberg, 1991).
[37] H. Reiss, C. S. Fuller, and F. J. Morin, Bell Syst. Tech. J. **35**, 535 (1956).
[38] H. Reiss, J. Appl. Phys. **30**, 1141 (1959).
[39] T. R. Waite, Phys. Rev. B **107**, 463 (1957).
[40] T. R. Waite, Phys. Rev. B **107**, 471 (1957).

[41]See, for example, W. Y. Yen, D. R. Johnson, and M. Dole, J. Phys. Chem. **78**, 1798 (1974).
[42]P. Ugliengo, see http://www.moldraw.unito.it for "MOLDRAW" (2006), a program to display and manipulate molecular crystal structures.
[43]See http://povray.org for "POV-Ray."
[44]F. Bekisli, W. B. Fowler, and M. Stavola, Phys. Rev. B **86**, 155208 (2012).
[45]O. W. Johnson, S.-H. Paek, and J. W. DeFord, J. Appl. Phys. **46**, 1026 (1975).
[46]J. B. Bates and R. A. Perkins, Phys. Rev. B **16**, 3713 (1977).
[47]J. B. Bates, J. C. Wang, and R. A. Perkins, Phys. Rev. B **19**, 4130 (1979).
[48]F. Filippone, G. Mattioli, P. Alippi, and A. Amore Bonapasta, Phys. Rev. B **80**, 245203 (2009).
[49]A. G. Marinopoulos, R. V. Vilão, H. V. Alberto, and J. M. Gil, J. Phys.: Condens. Matter. **30**, 425503 (2018).
[50]W. B. Fowler, A. Murphy, and M. Stavola, see http:meetings.aps.org/link/BAPS.2011.MAR.Q12.9 for an abstract on the dynamics of interstitial H in TiO_2.
[51]Herklotz *et al.,* Phys. Rev. B **108**, 205204 (2023).
[52]Hupfer *et al.,* Sci. Rep. **7**, 17065 (2017).